

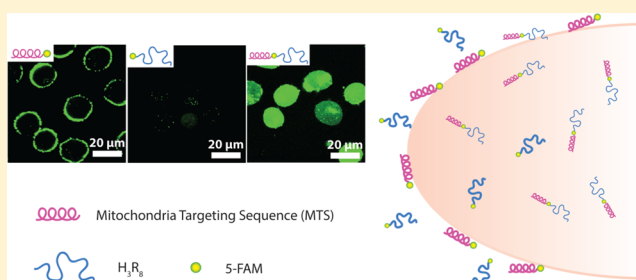
Dual Peptide Conjugation Strategy for Improved Cellular Uptake and Mitochondria Targeting

Ran Lin,^{†,‡} Pengcheng Zhang,^{†,‡} Andrew. G. Cheetham,^{†,‡} Jeremy Walston,[§] Peter Abadir,^{*,§} and Honggang Cui^{*,†,‡,⊥}

[†]Department of Chemical and Biomolecular Engineering, [‡]Institute for NanoBioTechnology, [§]Division of Geriatrics Medicine and Gerontology, and [⊥]Department of Oncology and Sidney Kimmel Comprehensive Cancer Center, The Johns Hopkins University, Baltimore, Maryland 21218, United States

Supporting Information

ABSTRACT: Mitochondria are critical regulators of cellular function and survival. Delivery of therapeutic and diagnostic agents into mitochondria is a challenging task in modern pharmacology because the molecule to be delivered needs to first overcome the cell membrane barrier and then be able to actively target the intracellular organelle. Current strategy of conjugating either a cell penetrating peptide (CPP) or a subcellular targeting sequence to the molecule of interest only has limited success. We report here a dual peptide conjugation strategy to achieve effective delivery of a non-membrane-penetrating dye 5-carboxyfluorescein (5-FAM) into mitochondria through the incorporation of both a mitochondrial targeting sequence (MTS) and a CPP into one conjugated molecule. Notably, circular dichroism studies reveal that the combined use of α -helix and PPII-like secondary structures has an unexpected, synergistic contribution to the internalization of the conjugate. Our results suggest that although the use of positively charged MTS peptide allows for improved targeting of mitochondria, with MTS alone it showed poor cellular uptake. With further covalent linkage of the MTS-5-FAM conjugate to a CPP sequence (R₈), the dually conjugated molecule was found to show both improved cellular uptake and effective mitochondria targeting. We believe these results offer important insight into the rational design of peptide conjugates for intracellular delivery.



INTRODUCTION

Mitochondria exhibit vital and lethal functions in both physiological and pathological conditions because they provide the most cellular energy and also function as a regulator of intrinsic pathway of apoptosis.¹ Recently, changes in mitochondria and their interaction with many proteins were found to be responsible for many diseases including neurodegeneration and cancer.^{2,3} Dysfunctional mitochondria are also known to have a profound impact on the development of a host of chronic and aging related conditions.⁴ Despite the great potential as a therapeutic target, only a few drugs are able to actually accumulate in mitochondria.³ Drug delivery systems that could transport therapeutic agents specifically into mitochondria are therefore of critical importance to fulfill this goal.

Current approaches for a successful mitochondrial targeting have been developed based on various mechanisms including lipophilic cations such as triphenyl phosphonium (TPP),⁵ mitochondria targeting signal peptide (MTS),^{6,7} protein transduction domain peptide (PTD),^{8,9} and DQAsomes-DNA complexes.¹⁰ Chemical conjugation of the therapeutic agent to a molecule with the ability to target mitochondria provides an effective strategy and has been used to deliver a great diversity of cargo into mitochondria,^{11–14} including small molecule

drugs,^{15,16} oligodeoxynucleotides,¹⁷ macromolecules,¹⁸ liposomes,¹⁹ and proteins.^{7,20,21} Among various targeting agents, mitochondria targeting sequence (MTS), the protein-sorting peptide consisting of typically 20–40 residues (a.k.a. protein tags), could arguably represent the best conjugation platform for targeted delivery of molecules into mitochondria because MTS has a well-proven role in guiding proteins into mitochondria and also because MTS can be specifically and precisely processed by mitochondrial processing proteinases (MPP) to release the delivered molecular cargo in the mitochondria. Despite the difference in amino acid sequence,¹⁸ all the mitochondria targeting sequences share the common amphipathic helical feature,²² and can be recognized by the same receptors and apparatus on the mitochondrial surface. Although precursor sequences derived from natural mitochondrial proteins exhibit high specificity in mitochondrial targeting, several reports have shown that naturally derived MTS peptides have lower levels of cellular uptake despite their amphipathic and positively charged nature.^{23,24} Therefore, an additional

Received: August 29, 2014

Revised: December 9, 2014

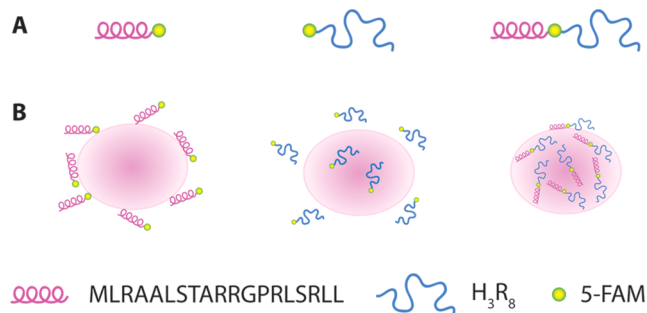
Published: December 30, 2014

feature must be included in the design to improve the intracellular access of MTS conjugates.

One widely used strategy to achieve effective intracellular access is to conjugate the therapeutic cargo with a cell-penetrating peptide (CPP)^{25–27} such as the HIV transactivator of transcription (Tat),^{28–32} penetratin,³³ and polyarginine.³⁴ It is generally accepted that positively charged CPP conjugates enter cells primarily through adsorption-mediated endocytosis pathways.^{35,36} Positive charge is a critical element for CPPs to exert successful membrane translocation,³⁷ as demonstrated by both protein derived CPPs such as Tat^{28,38,39} and *de novo* designed CPPs such as octaarginine (R₈).⁴⁰ Futaki et al. have shown that the “positive patch” of polyarginine played an essential role in peptide membrane permeability.⁴¹

To achieve improved mitochondrial targeting specificity and efficacy, we employed a dual peptide conjugation strategy that incorporates both CPP and MTS into one molecule. Notably, we found that the secondary structure of the conjugated peptides (both α -helices and polyproline II, PPII-like conformation) exhibits a synergistic effect on the cellular uptake of the resulting conjugate. Scheme 1 shows the

Scheme 1. Schematic Illustrations of (A) the Three Peptide Conjugates: MTS-5-FAM, 5-FAM-H₃R₈, and MTS-(5-FAM)-H₃R₈, and (B) Different Cellular Uptake of the Three Conjugates^a



^aMTS-5-FAM possessed α -helical secondary structure and showed no cell membrane-penetrating capability, but attaching to the cell membrane only. Cell penetrating peptide 5-FAM-H₃R₈ exhibited limited cellular uptake. Significant endocytosis was only observed for MTS-(5-FAM)-H₃R₈ containing both MTS and H₃R₈.

molecular design and peptide sequences of the three reported conjugates. The MTS peptide, MLRAALSTARRGPRLSRL, a well-studied natural presequence from the mitochondrial-oriented protein aldehyde dehydrogenase (ALDH), was selected as the mitochondrial targeting entity.^{42,43} The CPP R₈ was conjugated to this mitochondrial targeting system because of its remarkable ability to assist in cellular internalization. Three histidines (H₃) were introduced in the molecular design to offer the buffering effect upon protonation of the imidazole ring inside endosomes or lysosomes, which has been reported to induce the rupture of the endosomal/lysosomal membrane for the effective release of the entrapped conjugates into cytosols.^{44,45} 5-FAM was used as the fluorescent tracking agent due to its high quantum efficiency.⁴⁶

RESULTS AND DISCUSSION

Conjugate Characterization. The purities of the four studied conjugates were all above 90% according to analytical HPLC analysis (Supporting Information Figures S1–S4). The

observed multiply charged ions of MTS-5-FAM, 5-FAM-H₃R₈, MTS-(5-FAM)-H₃R₈, and 5-FAM-(RLL)₂R₈ suggest that the masses of the four conjugates were 2263.0, 2722.2, 4381.6, and 2616.6 Da, respectively, by ESI mass spectrometry, in agreement with the expected exact masses calculated for C₉₇H₁₄₇N₄₅O₂₀ (2263.5 Da), C₁₂₂H₁₉₆N₃₈O₃₁S (2723.2 Da), C₁₈₈H₃₁₃N₇₉O₄₂S (4381.5 Da), and C₁₁₅H₁₉₄N₄₈O₂₃ (2615.6 Da). Since the imidazole side-chain of histidine has an acid dissociation constant (pK_a) around 6, histidines under physiological conditions are not expected to be highly charged. Thus, 5-FAM-H₃R₈ carries more positive net charges at its arginine guanidinium groups (pK_a around 12) when compared with that of MTS-5-FAM. MTS-(5-FAM)-H₃R₈ and 5-FAM-(RLL)₂R₈ are expected to carry the most positive charges.

Cellular Uptake. We first used flow cytometry to investigate the cellular uptake efficacy of the three designed conjugates: 5-FAM-H₃R₈, MTS-5-FAM, and MTS-(5-FAM)-H₃R₈. In these experiments, cells were trypsinized to avoid false positive signals resulting from conjugates associated with the cell membrane via nonspecific electrostatic interactions.⁴⁷ Figure 1A reveals clearly that MTS-(5-FAM)-H₃R₈ shows

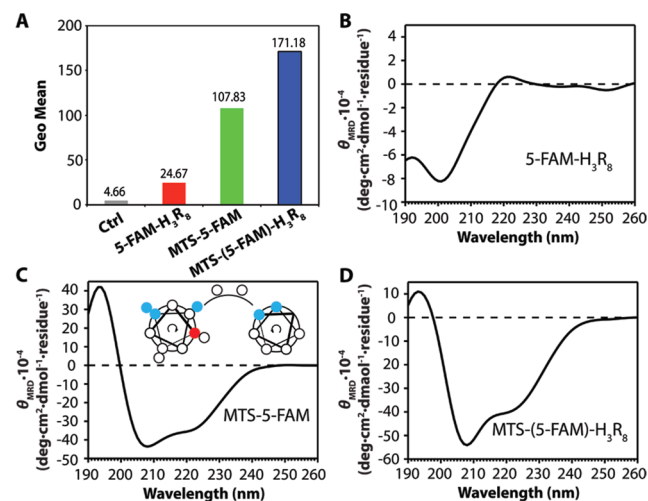


Figure 1. Representative flow cytometry results and circular dichroism (CD) spectra. (A) Quantitative comparison of the fluorescence intensity (in Geo mean) of three conjugates 5-FAM-H₃R₈ (red column), MTS-5-FAM (green column), and MTS-(5-FAM)-H₃R₈ (blue column) in MCF-7 breast cancer cell line after 4 h treatment with 1 μ M peptide conjugates, and untreated cells were used as control. CD spectra of (B) 50 μ M 5-FAM-H₃R₈, (C) 50 μ M MTS-5-FAM (Insertion: schematic illustration of positive charge distribution in MTS, red: methionine, blue: arginine.), and (D) 50 μ M MTS-(5-FAM)-H₃R₈. All the conjugates studied in CD analysis were dissolved in 20 mM sodium phosphate buffer (pH 7.4, with 20 mM SDS) at 37 $^{\circ}$ C.

superior cellular entry capability in comparison to both MTS-5-FAM and 5-FAM-H₃R₈, as evidenced by its strongest intensity (Supporting Information Figure S5). It is very surprising to see that MTS-5-FAM actually showed greater fluorescence intensity than 5-FAM-H₃R₈. Because increased positive charge would likely lead to improved cellular uptake against various cell lines via electrostatic interaction with negatively charged cell membranes,⁴⁸ one would expect a lower level of cellular uptake of MTS-5-FAM relative to that of 5-FAM-H₃R₈. The counterintuitive observation of higher fluorescence signal for MTS-5-FAM might be related to a difference in secondary

structures of MTS peptide versus R_8 , which is also known to play a role in cellular uptake. Schepartz et al. reported that cellular uptake of arginine-rich peptides was heavily dependent on the positive charge density, and the cellular uptake was enhanced when the arginines were clustered onto the same α -helical face.⁴⁹

We therefore performed circular dichroism experiments to investigate the secondary structures for all the synthesized conjugates. In order to mimic the hydrophobic environment in which peptide conjugates interact with cell membranes, peptide conjugates were dissolved in 20 mM sodium phosphate buffer with 20 mM sodium dodecyl sulfate (SDS) aqueous solution to obtain a 50 μ M solution (pH 7.4).^{50,51} The CD spectrum of 5-FAM- H_3R_8 was characterized by a minimum at 202 nm (Figure 1B), suggesting a PPII-like structure of H_3R_8 in a solution in the presence of SDS.⁵² The CD spectrum of MTS-5-FAM exhibited two minima at 208 and 222 nm (Figure 1C), in agreement with a typical CD absorption for peptides assuming α -helical conformation. This result is consistent with a previous report that the chosen MTS peptide could adopt two helices located at the N-terminal segment and C-terminal segment.⁴² As shown in Figure 1C inset, positive charges derived from arginine residues are clustered onto the same face within the α -helical arrangement, which may contribute to the greater fluorescence signal in flow cytometry for MTS-5-FAM. The CD spectrum of MTS-(5-FAM)- H_3R_8 reveals a similar α -helical structure that clearly originates from the MTS segment. The PPII-like structure from the CPP segment is likely to be overwhelmed by the signal of MTS due to its relatively lower CD absorption intensity (Figure 1D). To prove our assumption, we did a linear combination of the spectra collected from MTS-5-FAM and 5-FAM- H_3R_8 (Supporting Information Figure S6). As expected, the obtained spectrum predicts the spectrum from MTS-(5-FAM)- H_3R_8 well under the same conditions. It is also possible that higher cellular uptake of MTS-5-FAM compared with 5-FAM- H_3R_8 is due to the amphiphilic nature of the former molecule.

Intracellular Distribution. Given that flow cytometry only provides the overall fluorescence signals, we performed confocal imaging to study further the intracellular distribution of the endocytosed conjugates. As shown in Figure 2, cells treated with MTS-(5-FAM)- H_3R_8 showed intense green

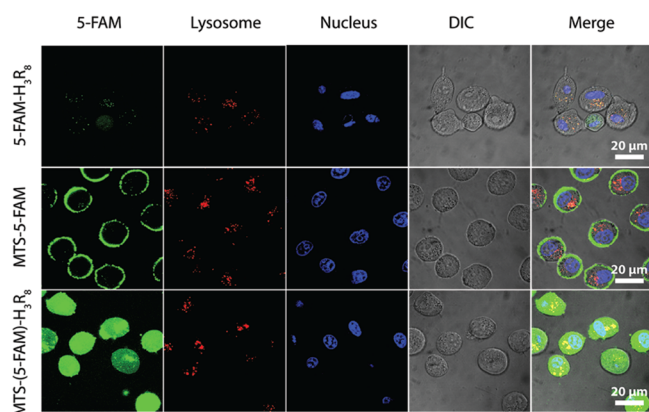


Figure 2. Cellular uptake of 5-FAM- H_3R_8 , MTS-5-FAM, and MTS-(5-FAM)- H_3R_8 in MCF-7 cells with lysosome (red, LysoTracker Red) and nucleus (blue, Hoechst 33342) after 4 h incubation with the respective conjugate (1 μ M). An enlarged image is also included in the Supporting Information (Figure S7).

fluorescence throughout the cytosol, suggesting efficient intracellular access and also successful endosomal/lysosomal escape. It is noteworthy that the intense green fluorescence observed from MTS-5-FAM treated cells does not stem from endocytosed conjugates but from molecules accumulated within cell membranes. It is very likely that the amphiphilic nature of MTS-5-FAM α -helices imparts the conjugate with a high propensity to insert into the cell membrane.^{52–55} These membrane entrapped conjugates cannot be simply removed by trypsinization, thus offering a very high fluorescent signal in the flow cytometry measurement. The tendency to stay within cell membrane may also explain the poor intracellular accumulation of MTS-5-FAM within MCF-7 cells. In contrast, the green fluorescence for cells treated with 5-FAM- H_3R_8 , albeit dim, arises primarily from within cells (Figure 2), implying both a low membrane accumulation tendency and poor cellular uptake efficiency. The difference in subcellular distribution of MTS-5-FAM and MTS-(5-FAM)- H_3R_8 leads us to speculate that effective entry into cytosols actually benefited from the combined use of an α -helical segment with a PPII-like unit in the MTS-(5-FAM)- H_3R_8 design, in which α -helical structures afford great binding affinity toward cell membrane while cell-penetrating segment H_3R_8 facilitates the entrance to the cytosols.

In order to verify our assumption that α -helical structures and PPII-like structures have synergetic effects in cellular uptake when used together, we designed and synthesized a new conjugate molecule 5-FAM-(RLL) $_2R_8$, in which the MTS peptide was replaced with a short α -helix forming peptide. Previous reports have suggested that a minimum of four α -helical arginines was required for efficient cell uptake.⁴⁹ The -RLLRLLR $_8$ - sequence was therefore chosen for the study, with arginines concentrated on the same face to resemble the secondary conformation of MTS-(5-FAM)- H_3R_8 . The secondary structure and cellular uptake of 5-FAM-(RLL) $_2R_8$ were investigated using the same conditions as the previous three conjugates.

The CD spectrum of 5-FAM-(RLL) $_2R_8$ confirmed the characteristic α -helical secondary structures, with two minima at around 208 and 222 nm, similar to that of MTS-(5-FAM)- H_3R_8 . The weak PPII-like structure signal was also overwhelmed by the negative absorption of α -helix at 208 as expected, resulting in a negative signal at \sim 200 nm. In order to compare intracellular uptake affected by secondary structures incorporated into the newly developed conjugate, flow cytometry was again performed to acquire quantitative results at the same conditions in previous study (Supporting Information Figure S8). As shown in Figure 3B, 5-FAM-(RLL) $_2R_8$ showed remarkably increased cellular uptake on MCF-7 breast cancer cells compared with that of 5-FAM- H_3R_8 (616 vs 24 in terms of geo mean fluorescence intensity). Since the only difference between the two studied molecules is the use of the α -helix forming peptide in 5-FAM-(RLL) $_2R_8$, these results clearly support our assumption that α -helical secondary structures exerted a synergistic effect on cellular uptake when used together with PPII-like structures.

Subcellular Colocalization. In order to evaluate if the dual-conjugated molecules are still capable of targeting mitochondria, we performed subcellular colocalization experiments. As shown in Figure 4, cells treated with MTS-5-FAM again showed intense 5-FAM green fluorescence only on the cell membrane, not within cells, that rarely overlaps with the Mitotracker signal. The overlap colocalization coefficients (S-

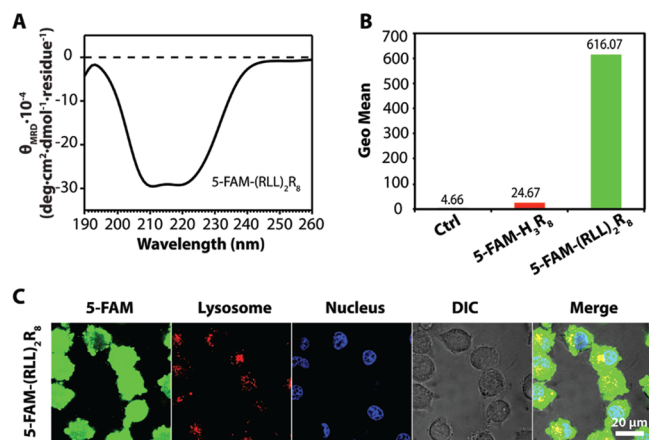


Figure 3. Investigation of secondary structure and its function performed on cellular uptake study of designed peptide conjugate 5-FAM-(RLL)₂R₈. (A) CD spectrum of 5-FAM-(RLL)₂R₈. (B) Representative flow cytometry results of 5-FAM-H₃R₈ (red column) and 5-FAM-(RLL)₂R₈ (green column). (C) Cellular uptake of 5-FAM-(RLL)₂R₈ in MCF-7 cells with lysosome (red, LysoTracker Red) and nucleus (blue, Hoechst 33342) after 4 h incubation with the conjugate (1 μM).

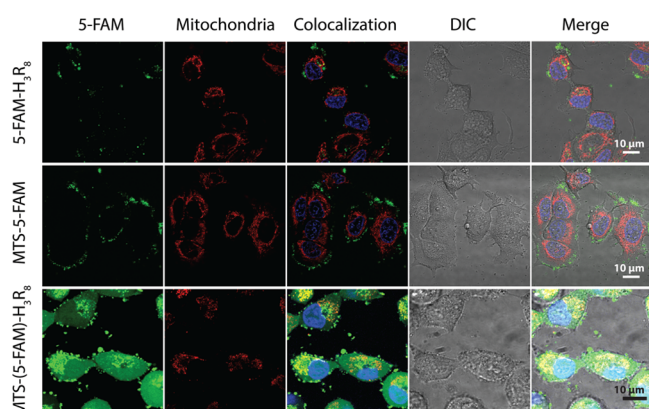


Figure 4. Subcellular colocalization of 5-FAM-H₃R₈, MTS-5-FAM, and MTS-(5-FAM)-H₃R₈ in MCF-7 cells with mitochondria (red, Mitotracker) and nucleus (blue, Hoechst 33342) after 2 h incubation of the respective conjugates (5 μM). An enlarged image is also included in the Supporting Information (Figure S9).

FAM and Mitotracker Red) were calculated to be 0.148 and 0.001 for 5-FAM-H₃R₈ and MTS-5-FAM, respectively, using the ZEN software with an intensity threshold of 10000. Cells treated with MTS-(5-FAM)-H₃R₈, when imaged using the same parameter settings, showed very intense green fluorescence throughout the cell. Although the deposition of conjugates in the cytosol is critical for further subcellular organelle targeting, it impedes the study of the conjugate's mitochondria targeting efficiency (all mitochondria appear to be colocalized with green signal from MTS-(5-FAM)-H₃R₈). As a consequence, the green signal has to be significantly attenuated to provide a clear vision, and only spots containing a very strong green signal remain visible, even though a partial colocalization of MTS-(5-FAM)-H₃R₈ green signal with Mitotracker was observed. The overlap colocalization coefficient (5-FAM and Mitotracker Red) were calculated to be 0.277 for MTS-(5-FAM)-H₃R₈ (Supporting Information Figure S10).

To exclude the possibility that the observed colocalization originated from the superposition of mitochondria with other conjugate-containing organelles such as lysosomes, we carefully analyzed our colocalization results and found that most of the conjugates were out of the lysosomes after 2 h incubation (Supporting Information Figure S11). We further performed the colocalization experiment on HeLa cells (human cervical cancer cell line) that are known to have a stretched morphology and less superposition between different subcellular organelles when cultured on a Petri dish. Obvious colocalization between MTS-(5-FAM)-H₃R₈ and mitochondria was noticed (Supporting Information Figure S12), which confirms the mitochondria targeting ability of the conjugate. Clearly, the MTS-(5-FAM)-H₃R₈ shows the highest targeting efficiency to mitochondria. However, as mentioned earlier, a significant amount of MTS-(5-FAM)-H₃R₈ was still out of mitochondria, which might be either trapped in endosomes/lysosomes (Figure 2) or en route to mitochondria. The relatively low colocalization efficiency could be due to the limited amount and capacity of translocase of the outer or inner mitochondrial membrane (TOM or TIM) complex that is primarily responsible for actively transporting cargos with MTS signal into mitochondria.⁵⁶ Another possibility for high cytosol retention might be the partial degradation of MTS-(5-FAM)-H₃R₈ in lysosomes during the intracellular transportation process, which could be potentially addressed in the future by use of MTS peptides of D-amino acids.

The mechanism of mitochondria accumulation of MTS-(5-FAM)-H₃R₈ is quite different from the Mitotracker used here or other triphenyl phosphonium (TPP) based targeting strategies which accumulate into mitochondria passively (therefore not saturable) due to their characteristic membrane potential.^{57,58} The MTS-(5-FAM)-H₃R₈ conjugate reported herein was expected to be transported into mitochondria through TOM/TIM complex. However, the resolution of fluorescent microscopy hinders the direct observation of their suborganelle distribution. Therefore, MitoBlock-6, an inhibitor of TOM/TIM complex, was used in the colocalization experiment to explore its effect on mitochondria transportation. Unexpectedly, we found that the use of MitoBlock-6 significantly limited the intracellular accumulation of MTS-(5-FAM)-H₃R₈ (Supporting Information Figure S13), which might be a result of inhibition in ATP production since MitoBlock-6 has been reported to affect the cytochrome C that is critical for ATP production.⁵⁹

Charged molecules or nanoparticles are known to disrupt cell membranes, thereby leading to increased intercellular uptake and possible cytotoxicity.⁶⁰ We therefore performed experiments to evaluate the potential cytotoxicity of all four conjugates against MCF-7 cell line. As shown in Figure 5, the four conjugates studied in this work did not reveal any noticeable toxicity behavior at 5 μM for a period of 4 h incubation, a concentration that was much higher than the concentration used for previous confocal imaging and flow cytometry experiments (1 μM).

CONCLUSION

In summary, we reported here a dual conjugate strategy to link a mitochondria targeting sequence, a cell penetrating peptide, and a non-membrane-penetrating dye into a conjugated molecule, and studied its cellular uptake and mitochondrial targeting behavior. Our results suggest that both α-helix and polyproline II-like structures are critical for facilitating the

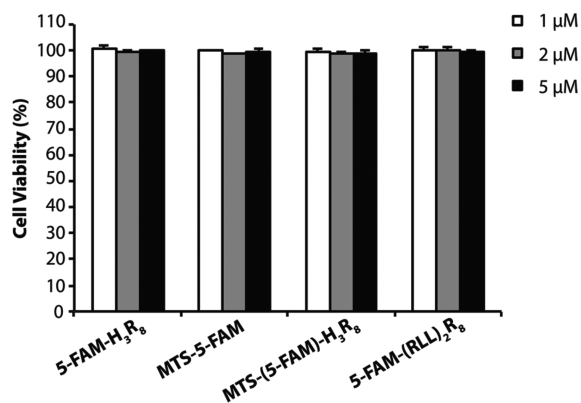


Figure 5. Cell viability of MCF-7 breast cancer cells after 4 h treatment with 5-FAM-H₃R₈, MTS-5-FAM, MTS-(5-FAM)-H₃R₈, and 5-FAM-(RLL)₂R₈ at three different concentrations (1, 2, and 5 μM). The results exhibited near nontoxicity of four conjugates at all three concentrations.

efficient cellular uptake of the conjugate, and when combined exert a synergistic effect. Although there are several parameters that require more rigorous evaluation and detailed studies, these results clearly demonstrate the great potential of using rationally designed peptide conjugates for intracellular delivery.

MATERIALS AND METHODS

Materials. All amino acids were purchased from Advanced Automated Peptide Protein Technologies (AAPPTEC, Louisville, KY) and Rink Amide MBHA Resin was purchased from NovaBiochem (San Diego, CA). 5-FAM was obtained from AnaSpec, Inc. (Fremont, CA), and all other reagents and solvents were sourced through VWR.

Cell Culture. MCF-7 cells were kindly provided by the Wirtz Lab (Department of Chemical and Biomolecular Engineering, Johns Hopkins University). Cells were cultured according to providers' protocols. MCF-7 human breast cancer cells were grown in DMEM with 10% fetal bovine serum (FBS, Invitrogen) and 1% antibiotics (Invitrogen). Cells were incubated at 37 °C in a humidified incubator with a 5% CO₂ atmosphere.

Conjugate Synthesis and Characterization. All peptide conjugates were synthesized using standard 9-fluorenylmethoxycarbonyl (Fmoc) solid phase synthesis techniques. The peptides Fmoc-K(Mtt)GH₃R₈-Rink, Fmoc-MLRA₂LSTAR₂GPRLSRL₂GK(Mtt)-Rink, Fmoc-MLRA₂LSTAR₂GPRLSRL₂K(Mtt)GH₃R₈-Rink, and Fmoc-K(Mtt)GRL₂RL₂R₈-Rink were synthesized on a 0.25 mmol scale on the Focus XC automated peptide synthesizer (AAPPTEC, Louisville, KY). For all peptide conjugates, 5-FAM was manually coupled at the peptide N- or C-terminus (after Mtt removal) with 5-FAM/HBTU/DIEA at a ratio of 4:4:10 relative to the peptide, shaken overnight at room temperature. Fmoc deprotections were performed using a 20% 4-methylpiperidine in DMF solution for 10 min and repeated once. Mtt deprotections were carried out using a mixture of TFA/TIS/DCM at a ratio of 4:5:91 for 5 min, repeating twice. Acetylation was performed on α-amino groups of N-terminus amino acids using a 20% acetic anhydride in DMF solution with 100 μL DIEA, shaken for 15 min, and the coupling was repeated once. In all cases, reactions were monitored by the ninhydrin test (Anaspec Inc., Fremont, CA) for free amines. Completed peptides were cleaved from the solid support using

a mixture of TFA/TIS/H₂O at a ratio of 92.5:2.5:5 for 2.5 h. Cold diethyl ether was added to precipitate the crude products, which were collected and dried under vacuum overnight.

All the conjugates were purified by preparative RP-HPLC using a Varian ProStar Model 325 HPLC (Agilent Technologies, Santa Clara, CA) equipped with a fraction collector. Separations were performed using a Varian PLRP-S column (100 Å, 10 μm, 150 × 25 mm) monitoring at 440 nm (for 5-FAM) and 220 (for peptide backbone). Collected fractions were analyzed by ESI-MS (LDQ Deca iontrap mass spectrometer, Thermo Finnigan, USA) and those containing the target molecules were combined and lyophilized (FreeZone -105 °C, Labconco, Kansas City, MO), and then stored at -4 °C.

The purity of all the conjugates was analyzed by HPLC using the following conditions: Agilent Zorbax-C18 column (5 μm, 4.6 × 150 mm); the flow rate was 1 mL/min, with the mobile phase starting from 5% MeCN (with 0.1% TFA) at 0 min to 95% MeCN (with 0.1% TFA at 25 min, and gradient changing back to the initial conditions at 26 min and holding at 5% MeCN for 4 min; the monitored wavelength was 220 nm. Peptide masses were determined by ESI-MS.

Circular Dichroism (CD) Measurement. To determine the peptide conformation, the CD spectra of all the conjugates (50 μM in 20 mM sodium phosphate buffer with 20 mM SDS) were recorded on a J-710 spectropolarimeter (JASCO, Easton, MD) from 190 to 260 nm, and the signal was converted from ellipticity (mdeg) to mean molar ellipticity per residue (deg·cm²·dmol⁻¹·residue⁻¹).

Cellular Uptake of Peptide Conjugates. To investigate the cellular uptake efficacy of the four designed conjugates, MCF-7 cells were seeded onto a 24-well plate at 1 × 10⁵ cells/well, and allowed to attach overnight. The medium was replaced with fresh medium containing the appropriate conjugate at 1 μM, and incubated with the cells for 4 h. The cells were then washed with DPBS twice, trypsinized, collected, washed twice with ice cold DPBS, and finally resuspended in 200 μL DPBS. The fluorescence intensity from endocytosed 5-FAM was analyzed using a FACScalibur flow cytometer (BD Biosciences, San Jose, CA) using the FL1 (530/30) channel.

Cytotoxicity. MCF-7 cells were seeded onto 96-well plate at 5 × 10³ cells/well, and allowed to attach overnight. The medium was replaced with fresh medium containing various concentrations of MTS-5-FAM, 5-FAM-H₃R₈, MTS-(5-FAM)-H₃R₈, or 5-FAM-(RLL)₂R₈, and incubated for 48 h. The cell viability was determined using the SRB method according to the manufacturer's protocol (TOX-6, Sigma, USA).

Subcellular Colocalization. The subcellular location of the endocytosed conjugates was investigated using confocal microscopy. Briefly, MCF-7 or HeLa cells were seeded onto an 8-well glass bottom plate (Labtek, Scott's Valley, CA) pretreated with type I rat tail collagen (Invitrogen) at 4 × 10⁴ cells/well, and allowed to attach overnight. For TIM/TOM complex inhibition study, cells were pretreated with 50 μM MitoBlock-6 for 15 min before conjugate addition. The cells were incubated with 5 μM peptide conjugates for 2 h. Thirty minutes before the washing step, 100 nM LysoTracker Red (Invitrogen) or Mitotracker Red (Invitrogen) was added with 10 μg/mL Hoechst 33342 (Invitrogen). The cells were then incubated in the phenol red free DMEM (Corning, Tewksbury, MA) supplemented with 10% FBS and imaged using a Zeiss 510 confocal laser scanning fluorescent microscope (Frankfurt, Germany).

■ ASSOCIATED CONTENT

■ Supporting Information

Additional characterization (HPLC, ESI-MS of the conjugates), cellular uptake of all the conjugates in MCF-7 cells, enlarged Figure 3 (intracellular distribution of MTS-5-FAM, 5-FAM-H₃R₈, MTS-(5-FAM)-H₃R₈ in MCF-7 cells) and Figure 5 (subcellular colocalization of MTS-5-FAM, 5-FAM-H₃R₈, MTS-(5-FAM)-H₃R₈ in MCF-7 cells), flow cytometry spectra, subcellular colocalization results in HeLa cells, and results of MCF-7 cells with MitoBlock-6 treatment can be found in online supporting material. This material is available free of charge via the Internet at <http://pubs.acs.org>.

■ AUTHOR INFORMATION

Corresponding Authors

*E-mail: pabadir1@jhmi.edu.

*Tel: (410)-516-6878. E-mail: hcu6@jhmi.edu.

Notes

The authors declare no competing financial interest.

■ ACKNOWLEDGMENTS

The work reported here is supported by National Science Foundation (DMR 1255281) and the Johns Hopkins University Claude D. Pepper Older Americans Independence Center, National Institute on Aging (NIA), P30AG021334. The authors thank Dr. Konstantopoulos (Department of Chemical and Biomolecular Engineering, Johns Hopkins University) and Dr. Hristova (Department of Materials Science and Engineering, Johns Hopkins University) for the use of their respective flow cytometer and the CD spectropolarimeter. We also thank the JHU Integrated Imaging Center (IIC) for the use of the confocal microscopy facility.

■ ABBREVIATIONS

5-FAM, 5-carboxyfluorescein; ALDH, aldehyde dehydrogenase; CD, circular dichroism; CPPs, cell penetrating peptides; DCM, dichloromethane; DIEA, diisopropylethylamine; DMEM, Dulbecco's modified eagle medium; DMF, *N,N*-dimethylformamide; DPBS, Dulbecco's phosphate buffered saline; FBS, fetal bovine serum; Fmoc, 9-fluorenylmethoxycarbonyl; HBTU, *O*-benzotriazole-*N,N,N'*-tetramethyluronium hexafluorophosphate; MeCN, acetonitrile; MTS, mitochondria targeting sequence; Mtt, 4-methyltrityl; ODN, oligodeoxynucleotide; PNA, peptide nucleic acid; PPII, Polyproline II; R₈, octaarginine; SDS, sodium dodecyl sulfate; SRB, Sulforhodamine B; Tat, transactivator of transcription; TFA, trifluoroacetic acid; TIS, triisopropylsilane

■ REFERENCES

- (1) Kroemer, G., Galluzzi, L., and Brenner, C. (2007) Mitochondrial membrane permeabilization in cell death. *Physiol. Rev.* 87, 99–163.
- (2) Lin, M. T., and Beal, M. F. (2006) Mitochondrial dysfunction and oxidative stress in neurodegenerative diseases. *Nature* 443, 787–795.
- (3) Fulda, S., Galluzzi, L., and Kroemer, G. (2010) Targeting mitochondria for cancer therapy. *Nat. Rev. Drug Discovery* 9, 447–464.
- (4) Abadir, P. M., Foster, D. B., Crow, M., Cooke, C. A., Rucker, J. J., Jain, A., Smith, B. J., Burks, T. N., Cohn, R. D., Fedarko, N. S., Carey, R. M., O'Rourke, B., and Walston, J. D. (2011) Identification and characterization of a functional mitochondrial angiotensin system. *Proc. Natl. Acad. Sci. U.S.A.* 108, 14849–14854.
- (5) Muratovska, A., Lightowers, R. N., Taylor, R. W., Turnbull, D. M., Smith, R. A. J., Wilce, J. A., Martin, S. W., and Murphy, M. P. (2001) Targeting peptide nucleic acid (PNA) oligomers to

mitochondria within cells by conjugation to lipophilic cations: implications for mitochondrial DNA replication, expression and disease. *Nucleic Acids Res.* 29, 1852–1863.

- (6) Mayer, A., Neupert, W., and Lill, R. (1995) Mitochondrial protein import - reversible binding of the presequence at the trans side of the outer-membrane drives partial translocation and unfolding. *Cell* 80, 127–137.

- (7) Schatz, G. (1996) The protein import system of mitochondria. *J. Biol. Chem.* 271, 31763–31766.

- (8) Schwarze, S. R., Hruska, K. A., and Dowdy, S. F. (2000) Protein transduction: unrestricted delivery into all cells? *Trends Cell Biol.* 10, 290–295.

- (9) Futaki, S. (2002) Arginine-rich peptides: potential for intracellular delivery of macromolecules and the mystery of the translocation mechanisms. *Int. J. Pharm.* 245, 1–7.

- (10) Weissig, V., D'Souza, G. G. M., and Torchilin, V. P. (2001) DQAsome/DNA complexes release DNA upon contact with isolated mouse liver mitochondria. *J. Controlled Release* 75, 401–408.

- (11) Yamada, Y., Akita, H., Kogure, K., Kamiya, H., and Harashima, H. (2007) Mitochondrial drug delivery and mitochondrial disease therapy - An approach to liposome-based delivery targeted to mitochondria. *Mitochondrion* 7, 63–71.

- (12) Jean, S. R., Tulumello, D. V., Wisnovsky, S. P., Lei, E. K., Pereira, M. P., and Kelley, S. O. (2014) Molecular vehicles for mitochondrial chemical biology and drug delivery. *ACS Chem. Biol.* 9, 323–333.

- (13) Kelley, S. O., Stewart, K. M., and Mourtada, R. (2011) Development of Novel Peptides for Mitochondrial Drug Delivery: Amino Acids Featuring Delocalized Lipophilic Cations. *Pharm. Res.* 28, 2808–2819.

- (14) Lei, E. K., Pereira, M. P., and Kelley, S. O. (2013) Tuning the intracellular bacterial targeting of peptidic vectors. *Angew. Chem., Int. Ed.* 52, 9660–9663.

- (15) Smith, R. A. J., Porteous, C. M., Coulter, C. V., and Murphy, M. P. (1999) Selective targeting of an antioxidant to mitochondria. *Eur. J. Biochem.* 263, 709–716.

- (16) Chamberlain, G. R., Tulumello, D. V., and Kelley, S. O. (2013) Targeted delivery of doxorubicin to mitochondria. *ACS Chem. Biol.* 8, 1389–1395.

- (17) Flierl, A., Jackson, C., Cottrell, B., Murdock, D., Seibel, P., and Wallace, D. C. (2003) Targeted delivery of DNA to the mitochondrial compartment via import sequence-conjugated peptide nucleic acid. *Mol. Ther.* 7, 550–557.

- (18) Del Gaizo, V., MacKenzie, J. A., and Payne, R. M. (2003) Targeting proteins to mitochondria using Tat. *Mol. Genet. Metab.* 80, 170–180.

- (19) Patel, N. R., Hatziantoniou, S., Georgopoulos, A., Demetzos, C., Torchilin, V. P., Weissig, V., and D'Souza, G. G. M. (2010) Mitochondria-targeted liposomes improve the apoptotic and cytotoxic action of sclereol. *J. Liposome Res.* 20, 244–249.

- (20) Torchilin, V. P. (2006) Recent approaches to intracellular delivery of drugs and DNA and organelle targeting. *Annu. Rev. Biomed. Eng.* 8, 343–375.

- (21) Yousif, L. F., Stewart, K. M., Horton, K. L., and Kelley, S. O. (2009) Mitochondria-penetrating peptides: sequence effects and model cargo transport. *ChemBioChem* 10, 2081–2088.

- (22) Vonhejine, G. (1986) Mitochondrial targeting sequences may form amphiphilic helices. *EMBO J.* 5, 1335–1342.

- (23) Karslake, C., Piotto, M. E., Pak, Y. K., Weiner, H., and Gorenstein, D. G. (1990) 2D NMR and structural model for a mitochondrial signal peptide bound to a micelle. *Biochemistry* 29, 9872–9878.

- (24) Pak, Y. K., and Weiner, H. (1990) Import of chemically synthesized signal peptides into rat-liver mitochondria. *J. Biol. Chem.* 265, 14298–14307.

- (25) Bode, S. A., Wallbrecher, R., Brock, R., van Hest, J. C. M., and Lowik, D. (2014) Activation of cell-penetrating peptides by disulfide bridge formation of truncated precursors. *Chem. Commun.* 50, 415–417.

- (26) Hansen, M. B., van Gaal, E., Minten, I., Storm, G., van Hest, J. C. M., and Lowik, D. (2012) Constrained and UV-activatable cell-penetrating peptides for intracellular delivery of liposomes. *J. Controlled Release* 164, 87–94.
- (27) Temming, R. P., Eggermont, L., van Eldijk, M. B., van Hest, J. C. M., and van Delft, F. L. (2013) N-terminal dual protein functionalization by strain-promoted alkyne-nitrone cycloaddition. *Org. Biomol. Chem.* 11, 2772–2779.
- (28) Frankel, A. D., and Pabo, C. O. (1988) Cellular uptake of the tat protein from human immunodeficiency virus. *Cell* 55, 1189–1193.
- (29) Zhang, P. C., Cheetham, A. G., Lin, Y. A., and Cui, H. (2013) Self-assembled Tat nanofibers as effective drug carrier and transporter. *ACS Nano* 7, 5965–5977.
- (30) Zhang, P. C., Cheetham, A. G., Lock, L. L., and Cui, H. G. (2013) Cellular uptake and cytotoxicity of drug-peptide conjugates regulated by conjugation site. *Bioconjugate Chem.* 24, 604–613.
- (31) Zhang, P. C., Lock, L. L., Cheetham, A. G., and Cui, H. G. (2014) Enhanced cellular entry and efficacy of Tat conjugates by rational design of the auxiliary segment. *Mol. Pharmaceutics* 11, 964–973.
- (32) Zhang, K., Fang, H. F., Chen, Z. Y., Taylor, J. S. A., and Wooley, K. L. (2008) Shape effects of nanoparticles conjugated with cell-penetrating peptides (HIV Tat PTD) on CHO cell uptake. *Bioconjugate Chem.* 19, 1880–1887.
- (33) Derossi, D., Chassaing, G., and Prochiantz, A. (1998) Trojan peptides: the penetratin system for intracellular delivery. *Trends Cell Biol.* 8, 84–87.
- (34) Mitchell, D. J., Kim, D. T., Steinman, L., Fathman, C. G., and Rothbard, J. B. (2000) Polyarginine enters cells more efficiently than other polycationic homopolymers. *J. Pept. Res.* 56, 318–325.
- (35) Lindgren, M., Hallbrink, M., Prochiantz, A., and Langel, U. (2000) Cell-penetrating peptides. *Trends Pharmacol. Sci.* 21, 99–103.
- (36) Copolovici, D. M., Langel, K., Eriste, E., and Langel, U. (2014) Cell-penetrating peptides: design, synthesis, and applications. *ACS Nano* 8, 1972–1994.
- (37) Ryser, H. J., and Hancock, R. (1965) Histones and basic polyamino acids stimulate the uptake of albumin by tumor cells in culture. *Science* 150, 501–3.
- (38) Wadia, J. S., Stan, R. V., and Dowdy, S. F. (2004) Transducible TAT-HA fusogenic peptide enhances escape of TAT-fusion proteins after lipid raft macropinocytosis. *Nat. Med.* 10, 310–315.
- (39) Green, M., and Loewenstein, P. M. (1988) Autonomous functional domains of chemically synthesized human immunodeficiency virus Tat trans-activator protein. *Cell* 55, 1179–1188.
- (40) Futaki, S., Suzuki, T., Ohashi, W., Yagami, T., Tanaka, S., Ueda, K., and Sugiura, Y. (2001) Arginine-rich peptides - An abundant source of membrane-permeable peptides having potential as carriers for intracellular protein delivery. *J. Biol. Chem.* 276, 5836–5840.
- (41) Futaki, S., Nakase, I., Suzuki, T., Youjun, Z., and Sugiura, Y. (2002) Translocation of branched-chain arginine peptides through cell membranes: flexibility in the spatial disposition of positive charges in membrane-permeable peptides. *Biochemistry* 41, 7925–7930.
- (42) Wang, Y., and Weiner, H. (1993) The presequence of rat-liver aldehyde dehydrogenase requires the presence of an alpha-helix at its N-terminal region which is stabilized by the helix at its C-termini. *J. Biol. Chem.* 268, 4759–4765.
- (43) Takayama, K., Nakase, I., Michiue, H., Takeuchi, T., Tomizawa, K., Matsui, H., and Futaki, S. (2009) Enhanced intracellular delivery using arginine-rich peptides by the addition of penetration accelerating sequences (Pas). *J. Controlled Release* 138, 128–133.
- (44) Varkouhi, A. K., Scholte, M., Storm, G., and Haisma, H. J. (2011) Endosomal escape pathways for delivery of biologicals. *J. Controlled Release* 151, 220–228.
- (45) Murphy, R. F., Powers, S., and Cantor, C. R. (1984) Endosome pH measured in single cells by dual fluorescence flow-cytometry - rapid acidification of insulin to pH-6. *J. Cell Biol.* 98, 1757–1762.
- (46) Fernandez-Suarez, M., and Ting, A. Y. (2008) Fluorescent probes for super-resolution imaging in living cells. *Nat. Rev. Mol. Cell Biol.* 9, 929–943.
- (47) Bailey, C. A., Miller, D. K., and Lenard, J. (1984) Effects of DEAE-dextran on infection and hemolysis by VSV. Evidence that nonspecific electrostatic interactions mediate effective binding of VSV to cells. *Virology* 133, 111–118.
- (48) Jiang, T. Y., Zhang, Z. H., Zhang, Y. L., Lv, H. X., Zhou, J. P., Li, C. C., Hou, L. L., and Zhang, Q. (2012) Dual-functional liposomes based on pH-responsive cell-penetrating peptide and hyaluronic acid for tumor-targeted anticancer drug delivery. *Biomaterials* 33, 9246–9258.
- (49) Appelbaum, J. S., LaRochelle, J. R., Smith, B. A., Balkin, D. M., Holub, J. M., and Schepartz, A. (2012) Arginine topology controls escape of minimally cationic proteins from early endosomes to the cytoplasm. *Chem. Biol.* 19, 819–830.
- (50) Lindberg, M., Jarvet, J., Langel, U., and Graslund, A. (2001) Secondary structure and position of the cell-penetrating peptide transportin in SDS micelles as determined by NMR. *Biochemistry* 40, 3141–3149.
- (51) Magzoub, M., Kilk, K., Eriksson, L. E. G., Langel, U., and Graslund, A. (2001) Interaction and structure induction of cell-penetrating peptides in the presence of phospholipid vesicles. *Biochim. Biophys. Acta, Biomembr.* 1512, 77–89.
- (52) Magzoub, M., Eriksson, L. E. G., and Graslund, A. (2002) Conformational states of the cell-penetrating peptide penetratin when interacting with phospholipid vesicles: effects of surface charge and peptide concentration. *Biochim. Biophys. Acta, Biomembr.* 1563, 53–63.
- (53) Eiriksdottir, E., Konate, K., Langel, U., Divita, G., and Deshayes, S. (2010) Secondary structure of cell-penetrating peptides controls membrane interaction and insertion. *Biochim. Biophys. Acta, Biomembr.* 1798, 1119–1128.
- (54) Park, C. B., Yi, K. S., Matsuzaki, K., Kim, M. S., and Kim, S. C. (2000) Structure-activity analysis of buforin II, a histone H2A-derived antimicrobial peptide: The proline hinge is responsible for the cell-penetrating ability of buforin II. *Proc. Natl. Acad. Sci. U.S.A.* 97, 8245–8250.
- (55) Duchardt, F., Fotin-Mleczek, M., Schwarz, H., Fischer, R., and Brock, R. (2007) A comprehensive model for the cellular uptake of cationic cell-penetrating peptides. *Traffic* 8, 848–866.
- (56) Neupert, W., and Herrmann, J. M. (2007) Translocation of proteins into mitochondria. *Annu. Rev. Biochem.* 76, 723–749.
- (57) Marrache, S., and Dhar, S. (2012) Engineering of blended nanoparticle platform for delivery of mitochondria-acting therapeutics. *Proc. Natl. Acad. Sci. U.S.A.* 109, 16288–16293.
- (58) Boddapati, S. V., D'Souza, G. G. M., Erdogan, S., Torchilin, V. P., and Weissig, V. (2008) Organelle-targeted nanocarriers: Specific delivery of liposomal ceramide to mitochondria enhances its cytotoxicity in vitro and in vivo. *Nano Lett.* 8, 2559–2563.
- (59) Dabir, D. V., Hasson, S. A., Setoguchi, K., Johnson, M. E., Wongkongkathep, P., Douglas, C. J., Zimmerman, J., Damoiseaux, R., Teitell, M. A., and Koehler, C. M. (2013) A small molecule inhibitor of redox-regulated protein translocation into mitochondria. *Dev. Cell* 25, 81–92.
- (60) Lovric, J., Bazzi, H. S., Cuie, Y., Fortin, G. R. A., Winnik, F. M., and Maysinger, D. (2005) Differences in subcellular distribution and toxicity of green and red emitting CdTe quantum dots. *J. Mol. Med.* 83, 377–385.